

residue<sup>32,33</sup> (Glu-270) in the cavity. Liver alcohol dehydrogenase has an anion binding site, about 15 Å from the metal, whose occupancy may account for the low affinity of a second anion for the metal.<sup>34,35</sup> Even transferrin, which requires carbonate to bind the metal, does not allow any other anion to bind to the metal ion.<sup>36</sup>

The decrease in the affinity of  $N_3^-$  among the SOD mutants here described strictly parallels the decrease in the superoxide dismutase activity. We speculate that the activity of the SOD enzyme depends on the affinity of the superoxide anion for the active cavity, i.e., that the decrease in activity is essentially due to an increase in  $K_m$  rather than to a decrease in  $k_{cat}$ . Only recently, have reliable values for  $k_{cat}$  and  $K_m$  been obtained:<sup>37</sup> measurements of this type are difficult to perform owing to the

difficulties in saturating the enzyme with  $O_2^-$ . A test of our hypothesis through  $K_m$  measurements on the mutants would be even more difficult to perform if their  $K_m$  values are indeed larger.

Our results support the view that superoxide does enter the active cavity and that the  $O_2^-$ -Cu<sup>II</sup> electron transfer is not a far away outer-sphere process. This does not necessarily mean that  $O_2^-$  must bind copper(II) in the same fashion as azide does, i.e., moving in the equatorial plane and displacing His-46. The substrate may pass its electron to copper(II) at an earlier stage, either through the semicoordinated water molecule or by removing it and weakly interacting with copper(II) in the axial coordination position.

**Acknowledgment.** We thank Dr. G. T. Mullenbach for discussions and I. Laria for technical assistance. Thanks are expressed to Dr. R. Rastelli for performing atomic absorption analyses. The 300-MHz <sup>1</sup>H NMR spectra have been recorded at the High Field NMR Center, CNR, Bologna, with the technical assistance of D. Macciantelli. This work has been performed with the contribution of the Progetto Strategico Biotecnologie del CNR and of Chiron Corporation.

**Registry No.** Arg, 74-79-3; Ile, 73-32-5; Lys, 56-87-1; Glu, 56-86-0; His, 71-00-1;  $N_3^-$ , 14343-69-2; Cu, 7440-50-8.

(32) Geoghegan, K. F.; Holmquist, B.; Spilburg, C. A.; Vallee, B. L. *Biochemistry* **1983**, *22*, 1, 47.

(33) Bicknell, R.; Schäffer, A.; Bertini, I.; Luchinat, C.; Auld, D. S.; Vallee, B. L. *Biochemistry* **1988**, *27*, 1050-1057.

(34) Olden, B.; Pettersson, G. *Eur. J. Biochem.* **1982**, *125*, 311-315.

(35) Bertini, I.; Lanini, G.; Luchinat, C.; Haas, C.; Maret, W.; Zeppezauer, M. *Eur. Biophys. J.* **1987**, *14*, 431-439.

(36) Chasteen, N. D. *Adv. Inorg. Biochem.* **1983**, *5*, 201-233.

(37) Fee, J. A.; Bull, C. *J. Biol. Chem.* **1986**, *261*, 13000-13005.

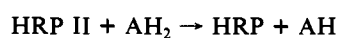
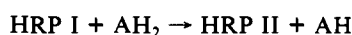
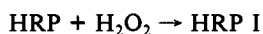
## Temperature Dependence and Electronic Transition Energies in the Magnetic Circular Dichroism Spectrum of Horseradish Peroxidase Compound I<sup>†</sup>

William R. Browett, Zbigniew Gasyna, and Martin J. Stillman\*

Contribution from the Department of Chemistry, University of Western Ontario, London, Ontario, Canada N6A 5B7. Received April 7, 1987

**Abstract:** Optical absorption and magnetic circular dichroism (MCD) spectra of horseradish peroxidase (HRP) compound I and HRP compound II have been recorded between 1.6 and 120 K. Above 30 K, the MCD spectrum of HRP compound I is dominated by temperature-independent transitions of the paramagnetic porphyrin  $\pi$ -cation-radical species. Below 30 K, temperature-dependent bands intensify until they dominate the MCD spectrum below 15 K and finally saturate below 2 K. This temperature dependence in the MCD spectrum is attributed to the effects of the  $S = 3/2$  Kramers' doublets ground state of the coupled Fe(IV) heme  $\pi$ -cation-radical species. Zero-field splitting in the  $S = 3/2$  ground state, which is calculated to be  $15 \pm 5 \text{ cm}^{-1}$ , results in a nonlinear temperature dependence in the MCD spectrum. In contrast, the temperature dependence in the MCD spectrum of HRP compound II is much less pronounced, and the intensity reaches a maximum between 25 and 30 K. This unique temperature dependence is associated with zero-field splitting that is estimated to be  $32 \pm 5 \text{ cm}^{-1}$ , for the Fe(IV),  $S = 1$ , ground state of the heme. Deconvolution calculations for both the MCD and the absorption spectra of the HRP and catalase compound I species are reported for the first time and provide meaningful data for the energies, intensities, and polarizations of the optical transitions. Little, if any, excited-state degeneracy is associated with the optical transitions in the experimental spectra of HRP or catalase compound I. The energies and intensities of the temperature-independent bands of HRP compound I are directly compared with those obtained in recent theoretical calculations that are based on Gouterman's four-orbital model and porphyrin  $\pi$ -cation-radical species. The results of the fitting procedure reveal that a single set of electronic transitions can account for the complete MCD and absorption spectral envelopes of both HRP and catalase compound I. These results indicate that the ground states in both the HRP and catalase compound I species should be considered to be admixtures of the  $^2A_{1u}$  and  $^2A_{2u}$  configurations, rather than an equilibrium mixture of configurations.

Horseradish peroxidase (HRP) (EC 1.11.1.7) catalyzes the oxidation of various substrates in the presence of  $H_2O_2$  by forming two sequential intermediates, HRP compound I and HRP compound II.<sup>1</sup> The compound I and II intermediates, which are two



and one oxidation equivalents above the native ferric heme, respectively, have been extensively studied.<sup>1-5</sup> Much of the previous work on this enzyme was undertaken in order to understand the role that these unusual heme electronic structures play in the

(1) Dunford, H. B.; Stillman, J. S. *Coord. Chem. Rev.* **1976**, *19*, 187-251.

(2) Dolphin, D.; Forman, A.; Borg, D. C.; Fajer, J.; Felton, R. H. *Proc. Natl. Acad. Sci. U.S.A.* **1971**, *68*, 614-618.

(3) Schulz, C. E.; Rutter, R.; Sage, J. T.; Debrunner, P. G.; Hager, L. P. *Biochemistry* **1984**, *23*, 4743-4754.

(4) Browett, W. R.; Stillman, M. J. *Biochim. Biophys. Acta* **1981**, *660*, 1-7.

(5) Chance, B.; Powers, L.; Ching, Y.; Poulos, T.; Schonbaum, G. R.; Yamazaki, I.; Paul, K. G. *Arch. Biochem. Biophys.* **1984**, *235*, 596-611.

<sup>†</sup>Publication No. 396 of the Photochemistry Unit, Department of Chemistry, University of Western Ontario.

enzymatic processes associated with the peroxidase and catalase enzymes. In agreement with the early descriptions of the electronic structure of these enzyme intermediates,<sup>2</sup> recent spectroscopic studies of HRP compound I have indicated that both oxidation equivalents are located on the heme that is in the form of a ferryl heme  $\pi$ -cation-radical complex and the single oxidation equivalent of HRP compound II is located on the iron in the heme that is in the form of a ferryl heme complex.<sup>3-5</sup> Phenomenological comparisons between the absorption and magnetic circular dichroism (MCD) spectra of  $\pi$ -cation-radical metalloporphyrin species<sup>6</sup> and the spectra of the HRP compound I and catalase compound I species, which were measured at 273 K,<sup>7</sup> have provided substantial support for this electronic arrangement. Comparison with the data obtained for the model compounds suggested that neither a distinct  ${}^2A_{2u}$  nor a  ${}^2A_{1u}$  ground state could give rise to the observed spectral data of the protein species.<sup>4</sup>

Despite the initial success in qualitatively assigning the general spectral features of compound I to those of a porphyrin  $\pi$ -cation radical and an oxoferryl (O=Fe<sup>IV</sup>) heme<sup>8-12</sup> species, the specific details of the electronic structure of the ferryl  $\pi$ -cation-radical heme ground state of HRP compound I remain controversial. ENDOR data for HRP compound I, which were measured at 4.2 K, have provided strong evidence for the characterization of HRP compound I as a low-spin ( $S = 1$ ) oxoferryl heme  $\pi$ -cation-radical complex.<sup>8,9</sup> These data also support the original suggestion<sup>2</sup> that the partially occupied orbital in the ground state has an  $a_{2u}$  symmetry, which gives a  ${}^2A_{2u}$  ground state. This assignment has also been suggested from NMR<sup>13,14</sup> and resonance Raman data.<sup>15</sup> However, the failure to recognize the well-documented photolability of the HRP compound I species<sup>16-20</sup> has been the source of conflicting analyses of the electronic structure of HRP compound I. The photolability of the protein is especially problematic when high-powered light sources, such as lasers,<sup>15,21,22</sup> are used. Furthermore, in order to correlate the analytical results from such a diverse set of techniques as EPR, ENDOR, and the resonance Raman spectroscopies with the structure and chemical properties of the protein in vivo, it has been necessary to assume that the electronic structure of the species studied under the temperature and glassing conditions used (frequently liquid helium temperatures) is directly related to that found under physiological conditions. It is important to note that, regardless of other conditions in the analysis, thermally activated structural changes, which can take place at the heme site as the temperature is reduced,<sup>23</sup> can

make this type of correlation highly tentative.

Under favorable circumstances, MCD spectroscopy can be used to link the results obtained at room temperature with those measured at liquid helium temperature, and these data can then be used to substantiate the correlations made by the different spectroscopic techniques described above. Also, because the MCD technique is sensitive to both the ground- and excited-state degeneracy of a chromophore, the magnetic field and temperature dependence in the MCD spectrum can provide valuable information concerning the chromophore's electronic structure that may not be obtainable by any other means. Initial studies, which were carried out in our laboratory, have shown that the MCD spectrum of HRP compound I<sup>20,24</sup> is temperature dependent. Temperature dependence has also been observed by us<sup>24</sup> and others<sup>25</sup> in the MCD spectrum of compound II.

The use of the  $\pi$ -cation-radical metalloporphyrins as models of the ground state of the compound I enzyme intermediates rests with Gouterman's four-orbital theoretical model,<sup>26-30</sup> which has successfully provided quantitative descriptions of the absorption and MCD spectra of porphyrins. Recently, the model has been extended to predict the absorption spectra of the  $\pi$ -cation-radical derivatives of porphyrins.<sup>31</sup> These calculations indicate that there should be distinct differences between the absorption spectra of the complexes that have either the  ${}^2A_{2u}$  or  ${}^2A_{1u}$ <sup>31</sup> ground-state configuration. Because the experimental absorption and MCD spectra of HRP and catalase compound I contain many overlapping bands,<sup>6,7</sup> a simple alignment of the dominant spectral features of these data to the theoretically calculated transition energies is unsatisfactory. A much more quantitative method is required.

In this paper, the MCD technique is used to investigate the electronic structures of the HRP compound I and compound II species through an analysis of the magnetic field and temperature dependencies of the MCD spectra. The deconvolution of sets of absorption and MCD spectra is proposed as a method to obtain meaningful reference data for the energy, intensity, and polarization of the optical transitions. On the basis of the results of these deconvolution calculations, a comparison of the electronic spectra of HRP compound I, catalase compound I, and the model porphyrins is made and related to the theoretical calculations for the electronic spectra of the metalloporphyrin  $\pi$ -cation radicals.<sup>31</sup> To our knowledge, there have been no previous systematic attempts to deconvolute the spectra of these important species into their constituent bands.

## Experimental Section

**Material and Methods.** Horseradish peroxidase (HRP; Boehringer Mannheim, lyophilized, grade 1) was dissolved in a 1:1 v/v solution of water (not buffered) and glycerol. The OD<sub>403</sub>/OD<sub>280</sub> ratio for this solution was 3.3, which indicates that this protein sample is dominated by isoenzyme C.<sup>32</sup> The HRP solution was pretreated with H<sub>2</sub>O<sub>2</sub> (1.2:1, mole ratio, H<sub>2</sub>O<sub>2</sub>/protein) and allowed to stand at room temperature for from 12 to 24 h before use. A second 1.2:1 mole ratio aliquot of H<sub>2</sub>O<sub>2</sub> was added to the solution at 273 K to form the compound I species. HRP compound II was prepared by the addition of 2 mol equiv of H<sub>2</sub>O<sub>2</sub> to a solution of HRP already containing 2 mol equiv of *p*-cresol, at pH 10. Aliquots of either the compound I or compound II solution were transferred rapidly to an aluminum cell and plunged into liquid nitrogen to

- (6) Browett, W. R.; Stillman, M. J. *Inorg. Chim. Acta* **1981**, *49*, 69-77.  
 (7) Browett, W. R.; Stillman, M. J. *Biochim. Biophys. Acta* **1980**, *623*, 21-31.  
 (8) (a) Roberts, J. E.; Hoffman, B. M.; Rutter, R.; Hager, L. P. *J. Biol. Chem.* **1981**, *256*, 2118-2121. (b) Rutter, R.; Hager, L. P. *J. Biol. Chem.* **1982**, *257*, 7958-7961.  
 (9) Roberts, J. E.; Hoffman, B. M.; Rutter, R.; Hager, L. P. *J. Am. Chem. Soc.* **1981**, *103*, 7654-7656.  
 (10) Penner-Hahn, J. E.; Eble, K. S.; McMurry, T. J.; Renner, M.; Balch, A. L.; Groves, J. T.; Dawson, J. H.; Hodgson, K. O. *J. Am. Chem. Soc.* **1986**, *108*, 7819-7825.  
 (11) Chance, B.; Powers, L.; Ching, Y.; Poulos, T.; Schonbaum, G. R.; Yamazaki, I.; Paul, K. G. *Arch. Biochem. Biophys.* **1984**, *235*, 596-611.  
 (12) Chance, M.; Powers, L.; Kumar, C.; Change, B. *Biochemistry* **1986**, *25*, 1266-1270.  
 (13) La Mar, G. R.; de Ropp, J. S. *J. Am. Chem. Soc.* **1980**, *102*, 395-397.  
 (14) La Mar, G. R.; de Ropp, J. S.; Smith, K. M.; Langry, K. C. *J. Am. Chem. Soc.* **1983**, *105*, 4576-4580.  
 (15) Oertling, W. A.; Babcock, G. T. *J. Am. Chem. Soc.* **1985**, *107*, 6406-6407.  
 (16) Stillman, J. S.; Stillman, M. J.; Dunford, H. B. *Biochem. Biophys. Res. Commun.* **1975**, *63*, 32-35.  
 (17) Stillman, J. S.; Stillman, M. J.; Dunford, H. B. *Biochemistry* **1975**, *14*, 3183-3188.  
 (18) Nadezhdin, A. D.; Dunford, H. B. *Photochem. Photobiol.* **1979**, *29*, 889-903.  
 (19) McIntosh, A. R.; Stillman, M. J. *Biochem. J.* **1977**, *167*, 31-37.  
 (20) Browett, W. R.; Gasyna, Z.; Stillman, M. J. *Biochem. Biophys. Res. Commun.* **1983**, *112*, 515-520.  
 (21) Van Wart, H. E.; Zimmer, J. *J. Am. Chem. Soc.* **1985**, *107*, 3379-3381.  
 (22) Teraoka, J.; Ogura, T.; Kitagawa, T. *J. Am. Chem. Soc.* **1982**, *104*, 7354-7356.

- (23) Browett, W. R.; Stillman, M. J. *Biophys. Chem.* **1984**, *19*, 311-320.  
 (24) (a) Browett, W. R.; Gasyna, Z.; Stillman, M. J. *Inorg. Chim. Acta* **1983**, *79*, 115-116. (b) Gasyna, Z.; Browett, W. R.; Stillman, M. J. *Biochemistry* **1988**, *27*, 2503-2509.  
 (25) Nozawa, T.; Kobayashi, N.; Hatano, M.; Ueda, M.; Sogami, M. *Biochim. Biophys. Acta* **1980**, *626*, 282-290.  
 (26) Gouterman, M. *J. Chem. Phys.* **1959**, *30*, 1139-1161.  
 (27) Gouterman, M. *J. Mol. Spectrosc.* **1961**, *6*, 138-163.  
 (28) Gouterman, M. *The Porphyrins*; Dolphin, D., Ed.; Academic: New York, 1978; Vol. III, pp 1-135.  
 (29) McHugh, A. J.; Gouterman, M. *Theor. Chim. Acta* **1972**, *24*, 346-370.  
 (30) Ceulemans, A.; Oldenhof, N.; Gorller-Walrand, C.; Vanquickenborne, L. G. *J. Am. Chem. Soc.* **1986**, *108*, 1155-1163.  
 (31) Edwards, W. D.; Zerner, M. C. *Can. J. Chem.* **1985**, *63*, 1763-1772.  
 (32) Shannon, L. M.; Kay, E.; Lew, J. Y. *J. Biol. Chem.* **1966**, *241*, 2166-2172.

glass the solution. The glassed sample was transferred into an Oxford Instruments CF 204 exchange gas optical cryostat precooled to 100 K. The temperature of the sample was monitored with the Oxford Instruments CLTS temperature sensor mounted on the cryostat. The absorption spectra were obtained by placing the sample and the cryostat into a Cary 17 spectrophotometer. MCD spectra were obtained by placing a second sample in an Oxford Instruments SM4 magnet that was mounted in a CD spectrometer built in this laboratory. The temperature of this sample was monitored with a Lake Shore Cryotronics Inc. carbon glass sensor attached to the sample cell. All spectra shown in this paper were automatically digitized as they were recorded and have had the appropriate base lines subtracted. Spectral manipulations were carried out with the program SPECTRA MANAGER.<sup>33</sup> The absorption spectra have been recalculated with scales of  $\epsilon$  ( $\text{cm}^{-1} \text{M}^{-1}$ ), and the MCD spectra are presented as  $\Delta\epsilon$  ( $\text{cm}^{-1} \text{M}^{-1} \text{T}^{-1}$ ). Depolarization of the circularly polarized light by the frozen sample was estimated by placing an aqueous solution of dextro[tris(ethylenediamine)cobaltic] trihydrate before and after the sample. The depolarization was estimated at below 10% over the spectral range studied, although no adjustments to the  $\Delta\epsilon$  values have been attempted. Similarly, no adjustments were made for the highly variable contraction of the glass with cooling.

**Calculations.** The conventions described by Piepho and Schatz<sup>34</sup> are used throughout this paper to describe the absorption and MCD parameters. The CD sign is positive when absorption for left circularly polarized light is greater than that for right circularly polarized light ( $\Delta A = A_L - A_R$ ). The spectral features, which are apparent in the MCD spectrum, are the temperature-independent  $A$  and  $B$  terms and the temperature-dependent  $C$  term. The magnetic field is defined as positive when it is parallel to the light propagation direction. In the linear limit ( $g\beta B/kT \ll 1$ , where  $g$  is the ground-state  $g$  factor and  $\beta$  is the Bohr magneton), and assuming the rigid-shift and Born-Oppenheimer approximations, the MCD band shape is described by eq 1, where all the

$$\Delta A' / \xi = \Delta\epsilon' c l / \xi = 152.5 B c l [A_1 [-\delta f(\xi) / \delta \xi] + (B_0 + C_0 / kT) f] \quad (1)$$

energies,  $\xi$ , are in reciprocal centimeters, the magnetic flux density  $B$  is in tesla, and  $A_1$ ,  $B_0$ , and  $C_0$  are the MCD band parameters of the MCD  $A$ ,  $B$ , and  $C$  terms, respectively. The absorption band shape equation is given by eq 2 if the dipole strength,  $D_0$ , is expressed in debye units. The

$$A / \xi = \epsilon c l / \xi = 326.6 D_0 f c l \quad (2)$$

parameter  $f(\xi)$  is the line-shape function,  $c$  is the concentration,  $l$  is the path length,  $k$  is the Boltzmann factor, and  $T$  is the temperature.

**Zero-Field Splitting Calculations.** The zero-field splitting value,  $\Delta E$ , was calculated from measurements of the MCD intensity at different temperatures. The MCD intensity,  $\Delta A$ , which was assumed to be a temperature-dependent function of a three-state model (with degeneracies of 4 and 2 for the  $S = 3/2$  state in compound I and degeneracies of 2 and 1 for the  $S = 1$  state of compound II), was taken to be linearly proportional to the magnetic field and inverse temperature. The field and temperature dependencies of  $\Delta A$  can be derived as shown in eq 3,<sup>35</sup> where

$$\Delta A(\xi) = [(c_1\alpha_1 + c_2\alpha_2) / kT + (b_1\alpha_1 + b_2\alpha_2)] B \quad (3)$$

$\alpha_1 = 1 / (1 + 2e^{-\Delta E / kT})$  and  $\alpha_2 = 2e^{-\Delta E / kT} / (1 + 2e^{-\Delta E / kT})$  are the Boltzmann populations of each of the states,  $c_1$  and  $c_2$  are coefficients of the temperature-dependent component, and  $b_1$  and  $b_2$  are coefficients of the temperature-independent component.

The  $\Delta E$  value, which provided the best fit to the data, was calculated by searching for  $\Delta E$  values between 1 and 100  $\text{cm}^{-1}$ . Each  $\Delta E$  was used to calculate the appropriate  $\alpha_1$  and  $\alpha_2$ , and then the  $c_1$ ,  $c_2$ ,  $b_1$ , and  $b_2$  coefficients of eq 3 were determined by the Gauss-Jordan elimination method<sup>36</sup> of a matrix solution.

**Saturation Calculations.** When  $g\beta B/kT \gg 1$ ,  $\Delta\epsilon$  of eq 1 becomes nonlinear as a function of  $B/T$  and eventually becomes independent of the field and the temperature, at which point the signal is said to be fully saturated. MCD saturation measurements can be carried out by monitoring the MCD intensity as a function of magnetic field and temperature. Saturation data are typically plotted as MCD intensity vs  $\beta B / 2kT$  and have been described by saturation expressions for allowed electronic transitions of axial molecules;<sup>37</sup> these expressions have been extended by Thomson and Johnson.<sup>38</sup> The saturation data, and the related saturation

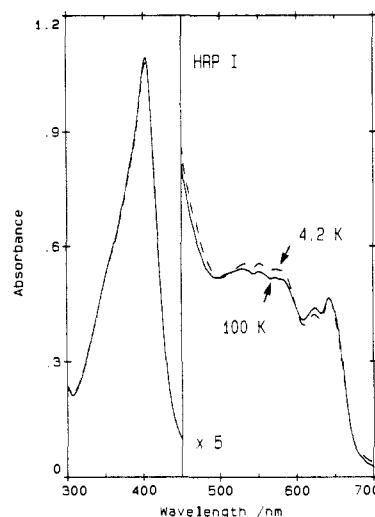


Figure 1. Optical absorption spectrum of HRP compound I at 100 K (solid line) and 4.2 K (broken line).

expressions,<sup>37,38</sup> can then be used to calculate the ground-state  $g$  factors for the lowest Kramers' doublet.

**Band-Fitting Calculations.** The spectral envelope fitting technique was based upon the use of general, nonlinear, least-squares and weighted-centroid SIMPLEX routines to provide the "best fit" to pairs of absorption and the MCD spectra of each complex.<sup>39</sup> The Gaussian line shape, which was selected as a reasonable approximation of the individual components that make up both the absorption and MCD spectra, can be described by  $f(\xi) = (1/\Delta\pi^{1/2})e^{-(\xi - \xi_0)^2/\Delta^2}$  and  $\Delta = \Gamma/2(\ln 2)^{1/2}$ , where  $\Gamma$  is the full width at half-height.<sup>37</sup>

## Results

**Temperature Dependence in the Absorption and MCD Spectra of HRP Compound I.** Figure 1 shows optical absorption spectra of horseradish peroxidase compound I at 100 and 4.2 K. These absorption spectra are very similar to the 273 K<sup>7</sup> and low-temperature<sup>40</sup> spectra previously published for HRP compound I. The broad series of overlapping transitions in the visible region are only slightly better resolved at 4.2 K. Similarly, the Soret band region remains dominated by an absorption band at 401 nm, which slightly increases in intensity in accordance with normal band-narrowing effects that are observed as a result of temperature reduction. The similarity of the absorption spectra over the full temperature range studied, and the similarity of the MCD spectra recorded at 273 and 100 K, suggests that the electronic configuration of HRP compound I is the same, or at least very similar, at both the high and low temperatures.

The series of broad overlapping bands in the absorption spectrum corresponds to a set of predominantly positive bands in the MCD spectrum, except in the 410- and 650-nm regions. These MCD spectral features differ markedly from those observed in the spectra of the high- and low-spin ferric porphyrins and hemes,<sup>41</sup> HRP compound II,<sup>7,40</sup> and the HRP compound I photochemical product.<sup>24</sup> Unlike data obtained in previous studies in which the HRP compound I spectra were contaminated by a small amount of photochemical product,<sup>20,42</sup> the MCD spectra, which were recorded between 1.6 and 100 K in this present study, show no indication of either HRP compound II or the HRP compound I photochemical product.

Figure 2 shows the combined effect of reducing the temperature from 92 to 3.5 K and varying the magnetic field from 4.56 to 1.27 T on the MCD spectrum of HRP compound I. The dramatic changes in MCD spectral intensity contrast sharply with the lack of change in the absorption data. The most spectacular effects

(33) Browett, W. R.; Stillman, M. J. *Comput. Chem.* **1987**, *11*, 73-82.  
(34) Piepho, S. B.; Schatz, P. N. *Group Theory in Spectroscopy*; Wiley: New York, 1983.

(35) Browett, W. R.; Fucaloro, A. F.; Morgan, T. V.; Stephens, P. J. *J. Am. Chem. Soc.* **1983**, *105*, 1868-1872.

(36) Miller, A. R. *Fortran Programs for Scientists and Engineers*; Sybex: Berkeley, 1983; pp 47-95.

(37) Schatz, P. N.; Mowery, R. L.; Krausz, E. R. *Mol. Phys.* **1978**, *35*, 1537-1557.

(38) Thomson, A. J.; Johnson, M. K. *Biochem. J.* **1980**, *191*, 411-420.

(39) Browett, W. R.; Stillman, M. J. *Comput. Chem.*, in press.

(40) Stillman, M. J.; Hollebone, B. R.; Stillman, J. S. *Biochem. Biophys. Res. Commun.* **1976**, *72*, 554-559.

(41) Dawson, J. H.; Dooley, D. M. *Iron Porphyrins. Part Three*; Lever, A. B. P., Gray, H. B., Eds.; Benjamin-Cummings: Reading, MA, 1985.

(42) Browett, W. R.; Gasyana, Z.; Stillman, M. J. *Inorg. Chim. Acta* **1983**, *79*, 113-114.

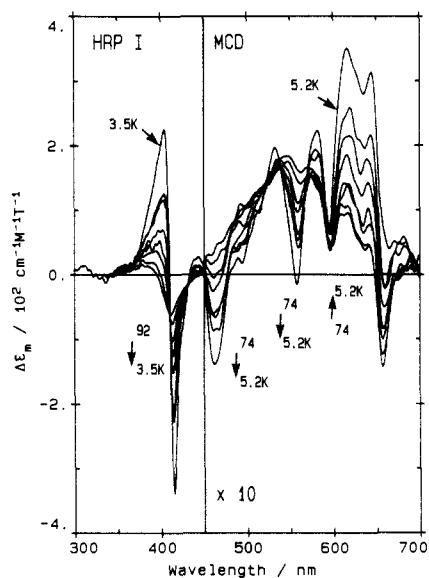


**Figure 2.** Effect of temperature on the MCD spectrum of HRP compound I. The temperatures range between 3.5 and 92 K. The spectra, which are normalized to 1 T and lie within the linear limit of the saturation curve, were recorded with magnetic fields between 1.27 and 4.56 T. For presentation purposes, the spectra in this plot were smoothed by using a FFT digital filter.

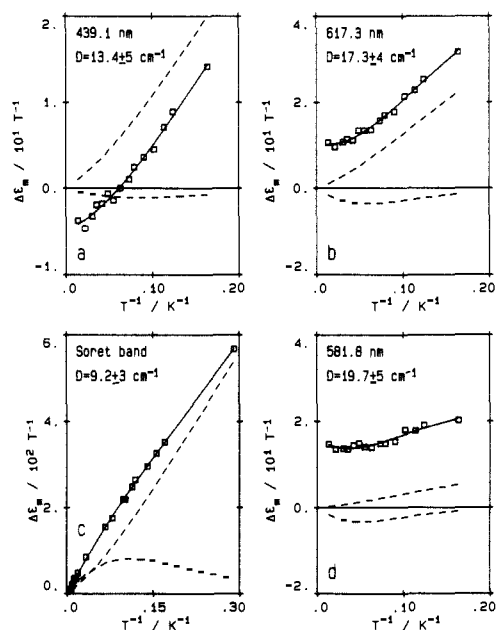


**Figure 3.** Inverse temperature dependence of the MCD signal intensities for HRP compound I at selected wavelengths. The observed data are presented as squares, the fit to the data is a solid line that is the sum of the temperature-dependent and -independent components, and the temperature-dependent components are represented by the dashed lines. For the Soret band, the peak-to-trough magnitude was used. An average zero-field splitting of  $15 \pm 5 \text{ cm}^{-1}$  was calculated.

occur in the red region of the MCD spectrum, where the characteristic negative band at 640 nm diminishes to zero as the temperature decreases. Figure 3 shows the dependence of the intensity on the inverse temperature ( $1/T$ ) of four selected bands in the MCD spectrum of HRP compound I. These temperature-induced changes are fully reversible. The nonlinear dependence, which is observed at temperatures that would normally be expected to give rise to a linear relationship, suggests that one or more low-lying degenerate excited states are thermally accessible and are close to a degenerate ground state. A change in the population across these degenerate states would then affect the temperature dependence of the MCD spectrum, if the  $C_0$ -term components differ, and, specifically, if  $c_1$  is not equal to  $c_2$  in eq

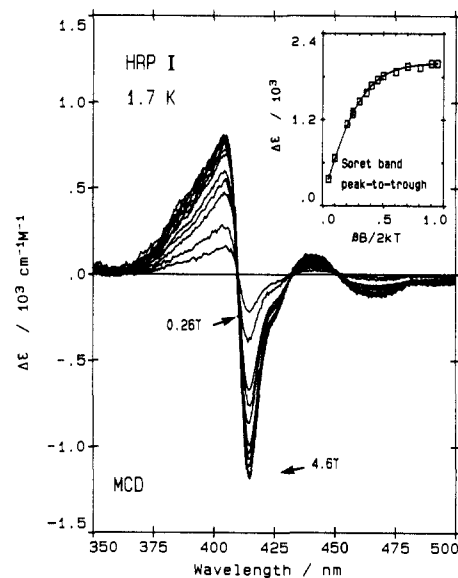


**Figure 4.** Series of spectra illustrating the effect of magnetic field on the MCD spectrum of HRP compound I at 1.7 K. The inset shows the magnetization curve that was obtained experimentally (squares) and the fitted function (solid line).

3. Our calculations, which assume a three-state model based on  $S = 3/2$  for HRP compound I and  $b_1 = b_2$  in eq 3 (i.e., the net  $B$ -term contribution is assumed to be temperature independent in these calculations), yield an average, zero-field splitting energy for the ground state of HRP compound I of  $15 \pm 5 \text{ cm}^{-1}$ . Calculations based on a two-state,  $S = 3/2$  model, in which each state has a degeneracy of 2, yield a zero-field splitting value of  $13 \pm 5 \text{ cm}^{-1}$ .

Figure 4 shows the magnetic field effect on the MCD spectrum of HRP compound I at 1.7 K. The magnetization curve for the B or Soret band, i.e., the band intensity (peak-to-trough) plotted vs  $\beta B/2kT$ , is presented in the inset. Increasing the magnetic field to a few tesla at this temperature results in the saturation of the signal intensity. The fit to the magnetization curve (solid line) was calculated by using theoretical expressions for a single Kramers' doublet of an iron porphyrin  $S = 3/2$  spin system described as eq 17 by Schatz.<sup>37</sup> If  $m_z = 0$  is assumed, then the curve is approximated by a slope of  $6.13 \times 10^3 \text{ M}^{-1} \text{ cm}^{-1}$  and a saturation limit of  $1.89 \times 10^3 \text{ M}^{-1} \text{ cm}^{-1}$  to produce an intercept value of  $I^{\text{exp}} = 0.316$  for the modified saturation expressions described by Thomson et al.<sup>38</sup> These saturation expressions give rise to a family of solutions for the  $g$  values for the HRP compound I heme group. By also assuming that  $g_{\text{par}} = g_z^{\text{eff}} = 2.0^3$  and  $g_{\text{perp}} = 3/(D \cdot I^{\text{exp}})^{38}$  we obtain  $g_{\text{perp}} \approx 4.8$ .

**Temperature Dependence in the Absorption and MCD Spectra of HRP Compound II.** Figure 5 shows optical absorption and MCD spectra of HRP compound II at 4.2 K. These spectra are typical of diamagnetic metalloporphyrins,<sup>41</sup> indicating that there is little interaction between the paramagnetic,  $S = 1$ , Fe(IV) and the diamagnetic ring  $\pi$ -electrons. However, the intensity of the MCD spectrum is still dependent on temperature. The inset in Figure 5 shows the effect of temperature on the MCD intensity of the Soret band (peak-to-trough) over the range 1.5–50 K. The fitted curve has been calculated by a two-state model that consists of a degenerate excited state (doublet,  $S_z = 1$ ) lying just above a nondegenerate (singlet,  $S_z = 0$ ) ground state of the  $S = 1$  iron(IV). Specifically, if  $c_1 = 0$  and  $b_1 \neq b_2$  in eq 3, a value for the zero-field splitting in HRP compound II of  $32 \pm 5 \text{ cm}^{-1}$  is found.

**Band-Fitting the Absorption and MCD Spectra of HRP Compound I.** The success of the band-fitting procedure stems from linking the individual bands in the absorption and MCD spectra;<sup>34</sup> specifically, calculations continue until a set of pairs of absorption and MCD bands, which have the same band center and related band shapes but may differ in intensity, have been found. Using such interrelated sets of the absorption and MCD spectra, we have

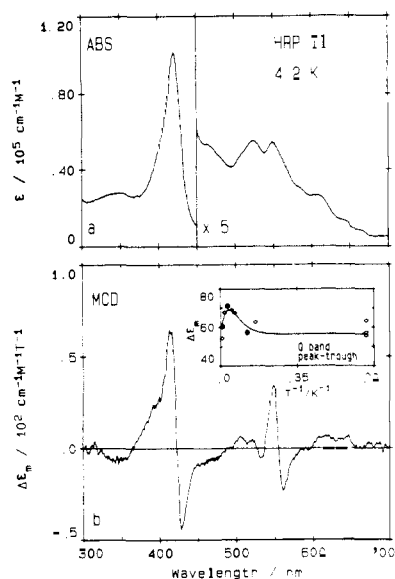


**Figure 5.** Optical absorption and MCD spectra of HRP compound I at 4.2 K. The inset shows the effect of temperature (1.50–125 K) on the Q-band MCD intensity. The observed Q-band peak-to-trough magnitudes are presented as squares, and the fit to this data, which is based on a zero-field splitting of  $32 \pm 5 \text{ cm}^{-1}$ , is a solid line and is the sum of the temperature-dependent and -independent components.

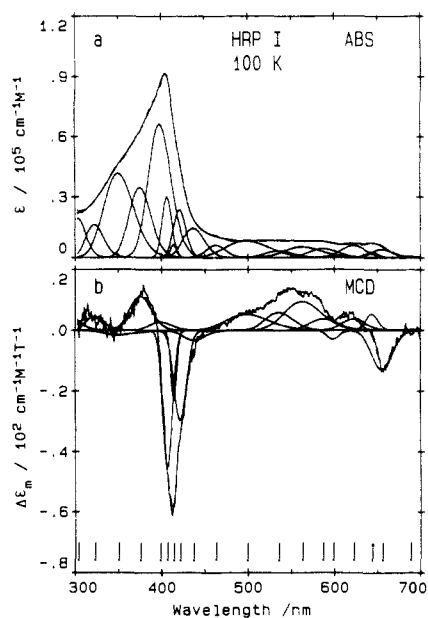


**Figure 6.** Results of the deconvolution calculations for a pair of absorption and MCD spectra of HRP compound I at 100 K. The individual band centers are listed in Table I. The vertical bars represent the band center positions of each of the calculated transitions. Note: the extinction coefficient depends on the thickness of the thin film at 100 K.

been able to produce meaningful fits to a number of porphyrin<sup>43</sup> and phthalocyanine neutral<sup>44a,b</sup> and  $\pi$ -cation-radical complexes.<sup>44a</sup>

Figure 6 shows the results of deconvolution calculations carried out for the pair of absorption and MCD spectra of HRP compound I obtained at 100 K. The set of bands used to fit the pair of spectra at 100 K also provided a very good fit to the 273 K spectra. The band center and oscillator strength for each band in the absorption

**Table I.** Theoretical Band Energies and Oscillator Strengths (in Parentheses) of Cobalt  $^2A_{2u}$   $\pi$ -Cation-Radical Porphine<sup>31</sup> Compared with Observed Band Positions and Intensities and Calculated Band Energies and Oscillator Strengths Found by Deconvolution of the Absorption and MCD Spectra of the  $^2A_{2u}$   $\pi$ -Cation-Radical Species<sup>6</sup> CoOEP<sup>2+</sup>,  $2\text{ClO}_4^-$  and HRP Compound I (Excited-State Symmetry of Theoretically Calculated States Presented in the Left-Hand Column)

$^2A_{2u}$ theory <sup>a</sup>	CoOEP <sup>2+</sup> , $2\text{ClO}_4^-$		HRP compd I (273 K)	
	obsd <sup>b</sup>	calcd <sup>c</sup>	obsd <sup>d</sup>	calcd <sup>e</sup>
		15.4 (0.006)		14.5 (0.021)
$^2E_g$ 14.7 (0.006)	15.7 (w)	15.9 (0.010)	15.5	15.3 (0.013)
				15.5 (0.002)
$^2E_g$ 15.5 (0.001)		16.8 (0.017)		16.1 (0.023)
		17.9 (0.039)		16.7 (0.003)
$^2A_{1g}$ 18.7 (0.009)	19.4 (m)	19.5 (0.037)	17.4	17.0 (0.023)
				17.8 (0.038)
		21.7 (0.058)		18.7 (0.016)
				20.0 (0.064)
				21.6 (0.024)
$^2E_g$ 19.5 (0.003)		23.7 (0.062)		22.9 (0.088)
$^2E_g$ 28.1 (0.165)		24.4 (0.044)		23.8 (0.062)
		25.2 (0.118) <sup>e</sup>		24.1 (0.008)
		25.7 (0.007)		24.6 (0.040)
$^2E_g$ 31.8 (3.252)	25.3 (s)	26.0 (0.512)	25.1 (s)	25.1 (0.394)
$^2A_{1g}$ 34.9 (0.029)	26.7 (sh)	27.9 (0.031)		26.6 (0.236)
$^2E_g$ 36.1 (0.021)		29.8 (0.191)	28.4 (sh)	28.5 (0.509)
$^2E_g$ 37.2 (0.075)	30.8 (w)	31.7 (0.219)		31.0 (0.140)
$^2A_{1g}$ 39.6 (0.009)		33.9 (0.225)		33.0 (0.151)
$^2E_g$ 40.8 (0.118)		38.6 (0.593)		

<sup>a</sup> From ref 31. Band centers are given in units of  $1000 \text{ cm}^{-1}$ . <sup>b</sup> From ref 6;  $\nu_{\text{max}}$  of the absorption spectrum. Intensity: (s) strong, (m) medium, (w) weak. <sup>c</sup> Calculated with band shape fitting programs to provide acceptable fits in both the absorption and the associated MCD spectrum. <sup>d</sup> Values obtained by measuring  $\nu_{\text{max}}$  in the absorption spectrum only. Intensity: (s) strong, (m) medium, (w) weak, (sh) shoulder. <sup>e</sup> Fit with an MCD  $A$  term.

**Table II.** Theoretical Band Energies and Oscillator Strengths (in Parentheses) of Cobalt  $^2A_{1u}$   $\pi$ -Cation-Radical Porphine<sup>31</sup> Compared with Observed Band Positions and Intensities and Calculated Band Energies and Oscillator Strengths Found by Deconvolution of the Absorption and MCD Spectra of the  $^2A_{1u}$   $\pi$ -Cation-Radical Species<sup>6</sup> CoOEP<sup>2+</sup>,  $2\text{Br}^-$  and Catalase Compound I<sup>4</sup> (Excited-State Symmetry of Theoretically Calculated States Presented in the Left-Hand Column)

theory <sup>a</sup>	CoOEP <sup>2+</sup> , $2\text{Br}^-$		catalase compd I (275 K)	
	obsd <sup>b</sup>	calcd <sup>c</sup>	obsd <sup>d</sup>	calcd <sup>e</sup>
$^2E_g$ 15.1 (0.095)	15.0 (m)	14.2 (0.012)		13.7 (0.043)
$^2A_{2g}$ 17.3 (0.001)	16.6 (w)	14.9 (0.031) <sup>e</sup>	15.1 (m)	14.8 (0.012)
$^2E_g$ 18.1 (0.042)		15.5 (0.017)		15.2 (0.016)
		16.3 (0.023)	16.7 (w)	16.1 (0.033)
				16.5 (0.000)
		17.1 (0.009)		17.0 (0.018)
		18.0 (0.016)		17.7 (0.038)
$^2A_{2g}$ 18.3 (0.015)	18.3 (w)	18.6 (0.000)	18.8 (w)	18.7 (0.021)
		19.5 (0.025)		20.2 (0.107)
		21.7 (0.061)		21.6 (0.063)
		23.4 (0.005)		22.8 (0.166)
$^2E_g$ 19.5 (0.000)		23.8 (0.093)		23.7 (0.104)
				24.2 (0.017)
$^2E_g$ 31.3 (1.908)	24.4 (m)	24.7 (0.019)		24.6 (0.447)
		25.7 (0.483)	24.9 (s)	25.1 (0.349)
				26.6 (0.242)
$^2E_g$ 33.2 (0.209)		28.7 (0.419)	28.6 (sh)	28.6 (0.555)
$^2A_{2g}$ 37.6 (0.016)		30.4 (0.104)		31.0 (0.237)
$^2E_g$ 37.7 (1.234)	29.4 (s)	31.8 (0.342)		33.0 (0.267)
$^2A_{2g}$ 38.9 (0.042)		34.7 (0.348)		
$^2E_g$ 39.2 (0.805)	35.1 (s)	39.1 (0.519)		
$^2E_g$ 41.8 (0.021)				

<sup>a</sup> From ref 31. Band centers are given in units of  $1000 \text{ cm}^{-1}$ . <sup>b</sup> From ref 6;  $\nu_{\text{max}}$  of the absorption spectrum. Intensity: (s) strong, (m) medium, (w) weak. <sup>c</sup> Calculated with band shape fitting programs to provide acceptable fits in both the absorption and the associated MCD spectrum. <sup>d</sup> Values obtained by measuring  $\nu_{\text{max}}$  in the absorption spectrum only. <sup>e</sup> Fit with an MCD  $A$  term.

(43) Gasya, Z.; Browett, W. R.; Stillman, M. J. *Porphyrins Excited States and Dynamics*; ACS Symposium Series 321; American Chemical Society: Washington, DC, 1986; pp 298–308.

(44) (a) Nyokong, T.; Gasya, Z.; Stillman, M. J. *Inorg. Chem.* **1987**, *26*, 1087–1095. (b) Ough, E.; Nyokong, T.; Creber, K. A. M.; Stillman, M. J. *Inorg. Chem.* **1988**, in press.

(45) Thomson, A. J.; Johnson, M. K.; Greenwood, C.; Gooding, P. E. *Biochem. J.* **1981**, *193*, 687–697.

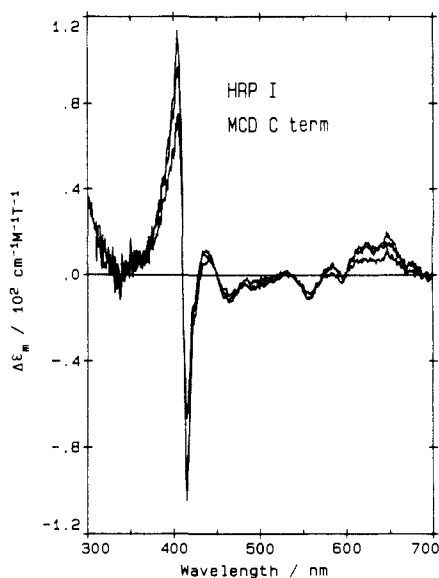


**Figure 7.** MCD C-term components in the spectrum of HRP compound I at 8.81 K (using a magnetic field of 1.53 T), 9.83 K (1.53 T), and 12.7 K (2.54 T). These spectra were calculated by subtracting from each spectrum the temperature-independent spectrum, which was measured at 100 K.

spectrum, and the sign of the MCD bands of HRP compound I at 273 K, are listed in Table I and graphically displayed in Figure 9.

A good fit to the catalase compound I absorption and MCD spectra<sup>4</sup> was achieved with a set of band parameters that is very similar to the HRP compound I set. The results are listed in Table II. Tables I and II also summarize the results of the deconvolution analysis for the spectra of HRP compound I, catalase compound I, the  ${}^2A_{2u}$  [CoOEP] $^{2+}2ClO_4^-$  species, and the  ${}^2A_{1u}$  [CoOEP] $^{2+}2Br^-$  species, as well as the corresponding theoretical calculations.<sup>31</sup> The model compound spectral data were fit independently of the protein data. Attempts to fit the porphyrin model compound spectra with a set of band parameters, which were similar to the band parameters of the HRP or catalase compound I data, produced poor results.

Figure 7 shows the individual, temperature-dependent components in the MCD spectrum of HRP compound I, which were extracted from the spectra recorded at several temperatures (about 8.8, 9.8, and 12.7 K). These components represent the MCD C-term bands of the spectrum. The MCD C terms, which according to eq 1 will have the shape of the MCD B term but are temperature dependent, were analyzed by band deconvolution techniques. Figure 8 presents the results of the deconvolution of the HRP compound I C-term components that are observed in the MCD spectrum recorded at 1.68 K.

## Discussion

**Zero-Field Splitting for  $S_1 = 1$  and  $S_2 = 1/2$  Spin-Coupled Systems.** The temperature dependence in the MCD spectral intensity of the heme serves as the basis for the determination of the saturation characteristics and the zero-field splitting parameters for both HRP compounds I and II. Qualitatively, the existence of the MCD C terms in the spectrum is a direct indication that coupling between the iron and the porphyrin is taking place in HRP compounds I and II.

A weak metal-porphyrin interaction is consistent with the low HRP compound I saturation limit. This saturation limit is significantly lower than the limits of well-characterized  $S = 1/2$  ferric heme complexes listed in Table III. This relatively low saturation value of  $1.9 \times 10^3 M^{-1} cm^{-1}$  is a reflection of a weaker spin-orbit coupling between the  $S = 1/2$  porphyrin radical and the  $S = 1$  Fe(IV) metal, in comparison with the coupling of the neutral porphyrin and the  $S = 1/2$  Fe(III) metal of other heme complexes.

The MCD saturation data for HRP compound I (Figure 4) can be described by equations<sup>37,38</sup> that involve ground-state  $g$

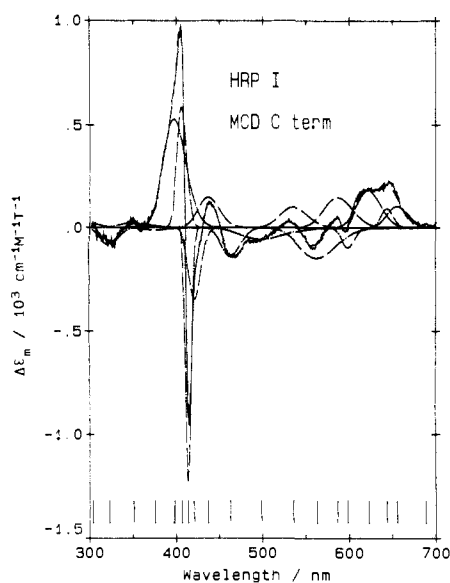


**Figure 8.** Results of deconvolution calculations for the C-term components in the MCD spectrum of HRP compound I at 1.68 K. This 1.68 K spectrum, which was recorded at 4.56 T, was calculated by subtracting the temperature-independent spectrum, which was recorded at 100 K, from the nearly saturated spectrum recorded at 1.68 K.

**Table III.** Saturation Limits of HRP Compound I Compared with Values Obtained for Several Low-Spin Ferric Heme Proteins<sup>a</sup>

compd	limit/ $10^3 M^{-1} cm^{-1}$	ref
HRP compound I	1.9	this work
horse heart cytochrome <i>c</i>	40.5	38
metmyoglobin CN <sup>-</sup>	60.5	38
cytochrome <i>c</i> oxidase	25	45
cytochrome <i>c</i> oxidase CN <sup>-</sup>	54	45

<sup>a</sup> The limit is measured as the peak-to-trough intensity of the Soret or B band of the MCD spectrum.

factors and transition dipole moments. If we assume for compound I, as in the EPR and Mössbauer calculations,<sup>3</sup> that the symmetry of the Fe(IV) is axially distorted from octahedral,  $g_{par} = g_z^{eff} = 2.0$ , and  $m_z = 0$ , then the saturation data for a Kramers' doublet from the  $S = 3/2$  ground state with axial symmetry are consistent with  $g_{perp} \approx 4.8$ . The  $m_z = 0$  assumption implies that the electronic transitions are completely *x* and *y* polarized. The  $g_{perp} \approx 4.8$  result is very sensitive to the model that is used to formulate the fitting equations, as well as to the quality of the data that are fitted, especially at high temperatures. Generally, because of the difference in state transitions involved between the resonance and optical techniques, considerable care should be taken in comparing parameters that are so symmetry dependent as  $g_{par}$  and  $g_{perp}$ . Clearly, as the extent of rhombicity increases, so the calculated value of  $g_{perp}$  from MCD data will degrade in accuracy. However, although analysis of EPR data for native, ferric HRP indicates a large degree of rhombic distortion so that  $g_x \neq g_y \neq g_z$ ,<sup>3</sup> analysis of the EPR and Mössbauer data for HRP compound I was carried out assuming only an axial distortion from octahedral symmetry and little rhombicity.<sup>3</sup> Although, the analysis of the EPR data for chloroperoxidase compound I<sup>3</sup> assumed considerable rhombic distortion.

For comparison of the  $g$  values obtained from the MCD spectral analysis we can look at the only other data available for compound I species, that is, the EPR and Mössbauer results for HRP compound I<sup>3</sup> and the EPR data of compound I of chloroperoxidase.<sup>8b</sup> Because of the limitations concerning the effect of unresolved symmetry distortions in all of these calculations, it is perhaps not surprising that our results do not confirm that the broad wings around the  $g_z^{eff} = 2$  EPR signal are from  $g_x$  and  $g_y$  of the HRP compound I species.<sup>3</sup>

At much higher temperatures, the complex temperature dependence of the HRP compound I MCD spectra is analyzed in terms of a zero-field splitting of a single manifold of Kramers

doublets. On the basis of the Mössbauer studies, the ground state of the HRP compound I heme has been described in terms of  $S = 1$  Fe(IV) that is spin coupled to a Kramers' doublet system with an  $S = 1/2$  from the  $\pi$ -cation radical. The zero-field splitting value for HRP compound I of  $15 \pm 5 \text{ cm}^{-1}$  was calculated as the average of the values that ranged from 9.2 to  $19.7 \text{ cm}^{-1}$  in Figure 3. This value is significantly lower than the value of  $\sim 26 \text{ cm}^{-1}$  (37 K) that was obtained from EPR experiments<sup>46,47</sup> although similar to  $18 \text{ cm}^{-1}$  (26 K) that was deduced from the Mössbauer experiment<sup>47</sup> and to values calculated for other peroxidase enzyme intermediates.<sup>3</sup> The accuracy of the zero-field splitting parameter calculation and this curve-fitting procedure depends on the quality of the data, and also on the unique shape contributions that can be provided by the  $c_1$  and  $c_2$  or  $b_1$  and  $b_2$  components in eq 3. The shapes of the temperature-dependent curves in Figure 3 result in the difference between the  $c_1$  and  $c_2$  components dominating the curve-fitting procedure. However, in Figure 3b-d there is a significant contribution to the intensity by a temperature-independent component. Inclusion of the MCD  $B$ -term contribution as  $b_1 \neq b_2$ , which might be expected to produce a  $b_1 = -b_2$  relationship,<sup>48</sup> in the fitting calculations did not produce meaningful results. Phenomenologically, if  $b_1$  is significantly different from  $b_2$ , this difference should be reflected in the shape of the temperature-dependent curve above 20 K. At the present moment, we do not know why  $b_1 \approx b_2$  rather than  $b_1 \neq b_2$ . However, the electronic coupling in the ground states of the HRP compound I species is very complicated and may not be described properly by previous theoretical models that were set up for quite different systems.<sup>48</sup>

An alternative explanation for the observed nonlinear inverse temperature dependence of the intensity of the MCD spectrum of HRP compound I, might be the multiple-state model that has been presented for the NMR data of model compounds.<sup>49</sup> In this model, there exists a thermal equilibrium between two slightly different electronic states and heme conformations,<sup>42,49,50</sup> which would result in different electronic couplings of the Fe(IV) with the porphyrin  $\pi$ -cation radical, each with a separate manifold of Kramers' doublets. However, this multiple-state equilibrium is not consistent with the results of the spectral-fitting calculations for HRP compound I that are presented below.

The very weak  $C$ -term contribution to the MCD spectrum of HRP compound II, shown in Figure 5, is fully consistent with a ground state that involves a degenerate excited state (doublet,  $S_z = 1$ ) lying just above a nondegenerate (singlet,  $S_z = 0$ ) ground state of the  $S = 1$  iron(IV). The combined effect of a rapid increase in intensity caused by the  $C$ -term component, and the decrease in population of this state as the temperature falls, is a temperature-dependent intensity profile that goes through a maximum at  $T \approx 30 \text{ K}$  and gives the value of the zero-field splitting of  $32 \pm 5 \text{ cm}^{-1}$ . The shape of the temperature-dependent profile is similar to that of the upper-state components of HRP compound I that are presented in Figure 3. This zero-field splitting value is larger than the value of  $22 \text{ cm}^{-1}$  that was obtained previously for HRP compound II and the myoglobin peroxide complex<sup>51</sup> and differs significantly from the value of  $12.5 \text{ cm}^{-1}$  for HRP compound II that was obtained with the Mössbauer spectroscopy.<sup>52</sup>

**Absorption and MCD Spectra of HRP Compound I.** The similarity of the spectral features of HRP compound I over the

100–273 K temperature range and the temperature dependence below 100 K indicates that the  $C$ -term component in the MCD spectrum, which is small at 100 K, is negligible at temperatures above 273 K. These results substantiate previous assumptions that the HRP compound I spectrum could be directly compared with the spectra of the model  $\pi$ -cation-radical species of porphyrins,<sup>4</sup> which have been produced by electrochemical,<sup>2</sup> chemical,<sup>6</sup> or photochemical oxidation in chlorinated solvents.<sup>53</sup>

The two models for the electronic configuration in the porphyrin  $\pi$ -cation radicals differ in the electron spin distribution around the porphyrin ring: For the  ${}^2A_{2u}$  radical, large spin density is placed on the meso carbons and the pyrrole nitrogens, whereas the  ${}^2A_{1u}$  radical has a small spin density at the meso carbon position.<sup>2</sup> Absorption and EPR spectra of porphyrin  $\pi$ -cation-radical model complexes have routinely been used to identify the radical species with either one of the two ground states, the  ${}^2A_{2u}$  or the  ${}^2A_{1u}$ .<sup>54</sup> Typically, the  ${}^2A_{2u}$  state has been assigned for the HRP compound I,<sup>8,15,55–58</sup> while  ${}^2A_{1u}$  has been assigned for the catalase compound I.<sup>2</sup> However, studies of models of HRP compound I have complicated the  ${}^2A_{2u}$  vs  ${}^2A_{1u}$  ground-state discussion by presenting evidence for a thermal equilibrium between the  ${}^2A_{2u}$  and  ${}^2A_{1u}$   $\pi$ -radical states<sup>50</sup> or data for a ruthenium meso heme analogue, which has been used to suggest that the electronic state of HRP compound I may have more  ${}^2A_{1u}$  than  ${}^2A_{2u}$  character.<sup>49,50</sup> Theoretical calculations of the electronic structure of models of HRP compound I have suggested that there should be a distinction between the  $A_{1u}$  and  $A_{2u}$  species,<sup>57,59</sup> although, because of the strong interaction between the two spin subsystems, it may be an over simplification to label HRP compound I as an " $a_{2u}$  cation radical".<sup>60</sup>

The theoretically predicted absorption spectra of the  $\pi$ -cation-radical derivatives of metalloporphyrins<sup>31</sup> indicate that the visible region of the spectrum of the  ${}^2A_{1u}$  species should consist of three separate bands that decrease in intensity with increasing energy, while that of the  ${}^2A_{2u}$  species should consist of three allowed transitions of nearly equal intensity. The Soret region of the  ${}^2A_{2u}$  ions should be dominated by one transition, while at least three strong bands are predicted in the Soret region for the  ${}^2A_{1u}$  cation radicals. The results from the deconvolution calculations carried out on the MCD and absorption spectra of the model porphyrin  $\pi$ -cation-radical species (Table I and II, Figure 9), the  ${}^2A_{2u} [\text{CoOEP}]^{2+}2\text{Br}^-$  and the  ${}^2A_{1u} [\text{CoOEP}]^{2+}2\text{Br}^-$  complexes, indicate that these  $\pi$ -cation-radical spectra are far more complicated than the theoretical calculations predicted.<sup>31</sup> Nonetheless, there appears to be reasonable alignment between these sets of data when the trends in oscillator strengths and transition energies are compared. A notable exception to this alignment is the predicted polarizations of the transitions (shown in the left-hand column of Tables I and II), which indicate that the MCD spectra should be dominated by MCD  $A$  terms. However, visual inspection of the MCD spectra and band-fitting results clearly indicate that porphyrin  $\pi$ -cation-radical MCD spectra are dominated by  $B$  terms. Attempts to fit these spectra with large numbers of  $A$  terms were not successful. Despite some scepticism in handling so many bands, recent calculations performed on spectra of the radical cation species of  $[\text{ZnPc}(-)]^{+\cdot}$ <sup>44a,61</sup> and  $[\text{MgPc}(-)]^{+\cdot}$ <sup>62</sup> in our laboratory suggest that

(53) Gasyana, Z.; Browett, W. R.; Stillman, M. J. *Inorg. Chem.* **1985**, *24*, 2440–2447.

(54) Fujita, I.; Hanson, L. K.; Walker, F. A.; Fajer, J. *J. Am. Chem. Soc.* **1983**, *105*, 3296–3300.

(55) Rutter, R.; Valentine, M.; Hendrich, M. P.; Hager, L. P.; Debrunner, P. G. *Biochemistry* **1983**, *22*, 4769–4774.

(56) Lang, G.; Boso, B.; Erler, B. S.; Reed, C. A. *J. Chem. Phys.* **1986**, *84*, 2998–3004.

(57) Hanson, L. K.; Chang, C. K.; Davis, M. S.; Fajer, J. *J. Am. Chem. Soc.* **1981**, *103*, 663–670.

(58) La Mar, G. R.; de Ropp, J. S.; Smith, K. M.; Langry, K. C. *J. Biol. Chem.* **1981**, *256*, 237–243.

(59) Loew, G. H.; Herman, Z. S. *J. Am. Chem. Soc.* **1980**, *102*, 6174–6175.

(60) Sontum, S. F.; Case, D. A. *J. Am. Chem. Soc.* **1985**, *107*, 4013–4015.

(61) Nyokong, T.; Gasyana, Z.; Stillman, M. J. *Inorg. Chem.* **1987**, *26*, 548–553.

(46) Schulz, C. E.; Devaney, P. W.; Winkler, H.; Debrunner, P. G.; Doan, N.; Chiang, R.; Rutter, R.; Hager, L. P. *FEBS Lett.* **1979**, *103*, 102–105.

(47) Colvin, J. T.; Rutter, R.; Stapleton, H. J.; Hager, L. P. *Biophys. J.* **1983**, *41*, 105–108.

(48) Collingwood, J. C.; Schwartz, R. W.; Schatz, P. N.; Patterson, H. H. *Mol. Phys.* **1974**, *27*, 1291–1317.

(49) Morishima, I.; Takamuki, Y.; Shiro, Y. *J. Am. Chem. Soc.* **1984**, *106*, 7666–7672.

(50) Morishima, I.; Shiro, Y.; Nakajima, K. *Biochemistry* **1986**, *25*, 3576–3584.

(51) Schulz, C. E.; Chiang, R.; Debrunner, P. G. *J. Phys. (Les Ulis, Fr)* **1979**, *40*, C2-534–C2J-536.

(52) Harami, T.; Maeda, Y.; Morita, Y.; Trautwein, A.; Gonser, U. *J. Chem. Phys.* **1977**, *67*, 1164–1169.

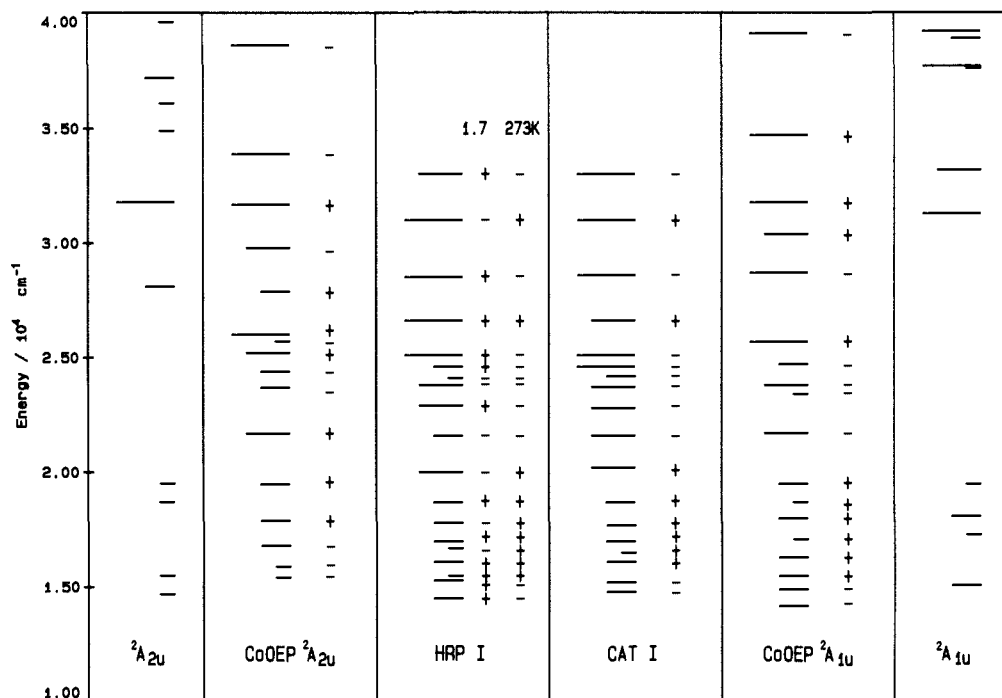


**Figure 9.** Energy level diagrams for the  ${}^2A_{2u}$  and  ${}^2A_{1u}$  ground states of theoretical models proposed for the porphyrin  $\pi$ -cation-radical species.<sup>31</sup> The predicted levels are compared with transition energies obtained from band-fitting pairs of absorption and MCD spectra of the cobalt octaethylporphyrin radical cations  $\text{Co}^{\text{III}}\text{OEP}^{2+}$ ,  ${}^2A_{2u}$ , and  $\text{Co}^{\text{III}}\text{OEP}^{2+}$ ,  ${}^2A_{1u}$ , (labeled  $\text{CoOEP } {}^2A_{2u}$  and  $\text{CoOEP } {}^2A_{1u}$ , respectively) and the HRP compound I (HRP I) and catalase compound I (CAT I) spectra. The sign of each band in each MCD spectrum is shown to the right of the bars. The four bar lengths indicate the relative oscillator strength of the transition (strong, intermediate, weak, and very weak). The two sets of signs for the MCD data of HRP compound I represent the signs of the MCD  $C$  terms (1.7 K) and  $B$  terms (273 K) of the transitions.

these calculations provide a reliable means of obtaining good band parameter data.

Significantly, the band-fitting procedure has produced a singlet set of band parameters that will describe the absorption and MCD spectra of the HRP compound I spectra throughout the temperature range studied in this work, as well as the catalase compound I spectra. The band parameters of the two protein species at 273 K (Tables I and II, Figure 9) differ in intensity but otherwise differ only slightly in band center or the presence of an additional minor band in the HRP compound I spectrum. Although the temperature-dependent component in the HRP compound I MCD spectrum appears to be dominated by a derivative-shaped spectral feature in the Soret region of the  $C$ -term component spectrum (Figures 7 and 8), this "A-term-like" feature is the result of two oppositely signed  $C$  terms which arise from nearly degenerate excited states that are subject to the same type of zero-field splitting as the ground state.<sup>63</sup> Unlike the protein spectra, the spectra of the cobalt porphyrin  $\pi$ -cation-radical complexes cannot be fit with a single set of bands.

The deconvolution of the HRP compound I spectra into a set of bands, which accounts for all the spectral features of the absorption and the MCD spectra over the entire temperature range, lends a great deal of support to the fitting results and indicates that all the major transitions in the porphyrin ring are affected by the interaction with the paramagnetic iron. No  $C$ -term components are observed in the MCD spectra of the zinc phthalocyanine  $\pi$ -cation-radical complex.<sup>44</sup>

Our study of the temperature dependence of the MCD spectrum of HRP compound I between 1.7 and 273 K indicates that HRP compound I consists of a single ground-state species, and therefore, there is no thermal equilibrium between  ${}^2A_{2u}$  and  ${}^2A_{1u}$  ground

states. However, significantly, the band-fitting results of both protein and model compound spectra do not allow an assignment of a distinct  ${}^2A_{2u}$  or  ${}^2A_{1u}$  ground state for either the HRP or catalase compound I species. The spectral data are consistent with a ground-state assignment that involves an admixture of the two distinct electronic structures.<sup>7,60</sup> However, the contributions of the two ground states may vary from protein to protein. For HRP compound I, there may be a preponderance of the  ${}^2A_{2u}$  ground state, as suggested by the similarity of band energies and MCD band signs, as illustrated in Figure 9. The similarity in the electronic structures, which is suggested by this analysis, for HRP compound I and beef liver catalase compound I implies that the differences in the electronic structures may be of little importance in determining the differences in the observed catalytic activity of the protein. The chemical properties and the stereochemistry of the heme pocket region may be much more important. This latter suggestion is consistent with recent work that has compared oxygen-carrying proteins with peroxidase enzymes according to the details of the stereochemistry of the heme site and their function.<sup>64,65</sup>

**Acknowledgment.** We acknowledge the financial support of this work by the NSERC of Canada through grants under the Operating, Equipment and Strategic (Energy) programs and from the Academic Development Fund at UWO (to M.J.S.). We also acknowledge very helpful comments made by Professor Andrew Thomson at the University of East Anglia. We are associated with the Centre for Chemical Physics and the Photochemistry Unit at UWO.

Registry No. Peroxidase, 9003-99-0.

(62) Ough, E.; Nyokong, T.; Stillman, M. J., unpublished results.  
 (63) Hatano, M.; Nozawa, T. *Adv. Biophys.* **1978**, *11*, 95-149.

(64) Poulos, T. L.; Kraut, J. *J. Biol. Chem.* **1980**, *255*, 8199-8205.  
 (65) Chance, M.; Powers, L.; Poulos, T.; Chance, B. *Biochemistry* **1986**, *25*, 1259-1265.